This article has been accepted for publication in IEEE Transactions on Biomedical Engineering. This is the author's version which has not been fully edited and content may change prior to final publication. Citation information: DOI 10.1109/TBME.2025.3589996

The Second Skin: A Wearable Sensor Suite that Enables Real-Time Human Biomechanics Tracking Through Deep Learning

Ryan T. F. Casey, Christoph P. O. Nuesslein, Felicia Davenport, Jason Wheeler, Anirban Mazumdar *Senior Member, IEEE*, Gregory Sawicki *Member, IEEE,* and Aaron J. Young *Senior Member, IEEE*

Abstract*—*Objective: **Real-time determination of human kinematics and kinetics could advance biomechanics research and enable valuable applications of biofeedback and generalizable exoskeleton control. This work aims to investigate a task-independent, user-independent method for obtaining precise real-time joint state estimation across lower-body joints during a wide variety of tasks.** ***Methods:*** **We developed a generalizable sensing approach using a suit comprised of inertial measurement units (IMUs) and pressure insoles. With the suit, we collected a dataset of 33 tasks commonly performed during construction and hazardous waste cleanup (N=10). We then trained deep learning user-independent, task-agnostic models to estimate joint lower-body kinematics and dynamics using only worn sensor data. We likewise computed joint kinematics and dynamics analytically from sensor data to serve as a comparison tool for model results.** ***Results:*** **Our models achieved overall angle estimation root-mean-squared-errors (RMSE) of 6.56±.92°, 8.60±1.01°, 7.58±.89°, and 6.00±.73° compared to 13.9±.1.3°, 15.31±1.0°, 10.76±.70°, and 7.56±.48° via analytical methods at the lower back, hip, knee, and ankle, respectively. Likewise, our models achieved overall normalized moment estimation RMSEs of .207±.069 Nm/kg, .242±.044 Nm/kg, .202±.038 Nm/kg, and .193±.034 Nm/kg compared to .306±.036 Nm/kg, .407±.021 Nm/kg, 1.18 ±.022 Nm/kg, and 1.73±.071 Nm/kg via analytical methods at the lower back, hip, knee, and ankle, respectively.** ***Conclusion:*** **These results are comparable to other state-of-the-art wearable sensing systems, establishing deep learning as a viable sensing approach that generalizes to new users and tasks.** ***Significance:*** **This work shows promise for enabling accurate real-world biomechanical data collection and enhancement of biofeedback systems and wearable robot control.**

***Index Terms*— Deep learning, Wearable systems and sensors, Joint biomechanics**

This work was supported by the U.S. Department of Energy's Office of Environmental Management. (Corresponding author: Ryan Casey)

Ryan Casey, Christoph Nuesslein, Anirban Mazumdar, Gregory Sawicki, and Aaron Young are with the Woodruff School of Mechanical Engineering, and the Institute for Robotics and Intelligent Machines, Georgia Institute of Technology, Atlanta, GA 30332 USA (e-mail: rcasey9@ gatech.edu).

Felicia Davenport is with the Woodruff School of Mechanical Engineering, Georgia Institute of Technology, Atlanta, GA 30332 USA

Jason Wheeler is with the Advanced Field Ops and Robotics division of Sandia National Laboratories, Albuquerque, NM, 87185 US

This article has supplementary downloadable material available at https://doi.org/---, provided by the authors. Digital Object Identifier ---

I. INTRODUCTION

REAL-TIME wearable sensing has the potential to revolutionize the fields of biomechanics and wearable robotics by enabling data collection in real-world settings, beyond the limitations of traditional lab environments. This framework preserves natural movements patterns and provides near-instantaneous biomechanical measurement, enabling wearable robots or biofeedback systems to act on real time information. Additionally, it greatly reduces the post-processing time needed to achieve usable data. These advantages make wearable sensing an attractive option for improving the safety of manual labor, for which traditional biomechanics methods would be impractical for wide-spread adoption. Moreover, there is a high prevalence of musculo-skeletal injuries in manual labor due to overexertion [1],[2] and a myriad of wearable assistive devices that have been developed to help reduce these injuries [3]. This necessitates the need for a broadly deployable wearable sensing layer that can monitor the biomechanics of manual laborers and enhance the capabilities of assistive devices. Many groups have developed devices and methods for wearable biomechanics sensing across a wide range of application areas [4],[5]. However, replicating the consistency and accuracy of optical motion capture and force plates, which are considered to be the state-of-the-art method for characterizing human movement [6], remains a pertinent challenge for all wearable systems.

Many wearable systems that rely on analytical methods for calculating joint states have been attempted. For kinematic sensing, angular measurement via strain sensors [7],[8] and via IMUs [9],[10] have been investigated. However, none have consistently performed with joint angle root mean square error (RMSE) below 5°, which is the standard for most applications [11]. For joint moment tracking, EMG-driven forward dynamics methods have been attempted [12],[13], however, EMG is highly variable across individuals and experimental sessions, making repeatable estimates of muscle forces from EMG sensors a major challenge [14-16]. Analytical inverse dynamics methods that attempt to infer all of the information typically provided by force plates (3 DOF forces and 3 DOF moments) from pressure insoles using simplistic models have also been attempted [17-19]. However, these methods generalize poorly to new tasks and users, and cannot rely on fully wearable kinematic tracking, because joint to joint error propagation drastically throws off joint moment results when moving up in the proximal chain from the ground. Of all these methods, IMUs and pressure insoles appear to be the most

Authorized licensed use limited to: Georgia Institute of Technology. Downloaded on October 31,2025 at 21:04:24 UTC from IEEE Xplore. Restrictions apply.
© 2025 IEEE. All rights reserved, including rights for text and data mining and training of artificial intelligence and similar technologies. Personal use is permitted, but republication/redistribution requires IEEE permission. See https://www.ieee.org/publications/rights/index.html for more information.

This article has been accepted for publication in IEEE Transactions on Biomedical Engineering. This is the author's version which has not been fully edited and content may change prior to final publication. Citation information: DOI 10.1109/TBME.2025.3589996

reliable wearable sensor combination for quantifying kinematics and kinetics, respectively, however, analytical methods alone have not proven to be sufficient for wearable biomechanics sensing.

More recently, machine learning has been able to surpass the shortcomings of analytical methods by virtue of its ability to find underlying patterns within time-series sensor data. Techniques including extreme gradient boosting (XGBoost), neural networks (NNs), convolutional neural networks (CNNs), temporal convolutional networks (TCNs), recurrent neural networks (RNNs), long short-term memory networks (LSTMs) and transformers have all previously been shown to estimate joint states [20-28]. Crucially, these approaches have succeeded using only inertial and force-sensing wearable device data, with some work even showing promise with subject-independent models (validation subject withheld from training data) or task-agnostic models (same model used across all tasks). However, existing work is limited both in terms of the number of joints and constituent states estimated, as well as the number of task types investigated. Furthermore, much of the work in this area involves devices that are complicated to don or require precise sensor placement, both of which are major drawbacks to real-world implementation. Thus, to enable accessible real-time estimates of complex joint states, the capabilities of a combined deep learning model and robust, easy-to-use sensing system is explored.

In this study, we developed an open-source wearable sensing suit that utilizes IMUs and pressure insoles along with a deep learning approach to be a practical solution for characterizing lower-body biomechanics in real time. We trained subject-independent, task agnostic models to estimate joint biomechanics across a wide array of tasks that manual laborers routinely perform. Then, we compared the joint state estimates from this approach to analytical methods of quantifying the same joint states from wearable sensors. We hypothesized that our deep learning approach would significantly outperform analytical methods, on a user-independent, task-agnostic basis, because it would account for inaccuracy and inconsistency from sensors.

This paper makes the following critical contributions to the field: 1) We demonstrate that deep learning combined with a large and diverse dataset enables accurate and real-time (every 5 ms) estimates of human kinematics and dynamics without the need for subject-specific or task-specific models. 2) We open source the 'Second Skin' design – a sensing layer that can provide out-of-the-lab biomechanics collections, real-time biofeedback, or input to a wearable robot for control applications. 3) We open source our dataset which provides a huge array of useful data of numerous industry-relevant tasking biomechanics and synced wearable sensing data for further development of data-driven systems.

II. Methods

A. The Second Skin

The Second Skin is an open-soruce wearable sensing device that comprises XSENSOR X4 high-resolution pressure insoles with attached IMUs at the feet (XSENSOR Technology Corporation, Calgary, AB Canada), as well as 6-axis IMUs at the shanks, thighs, pelvis and back (3DM-GX5-25, HBK MicroStrain, Williston, VT, USA) (Fig 1A). Each pressure insole provides vertical GRF (vGRF) and center-of-pressure (COP) readings while the IMUs provide orientation, linear acceleration and angular velocity. The pressure insoles are worn in the shoes, while the shank, thigh, and pelvis IMUs are strapped to Velcro sewn onto compression pants to achieve skin-level contact with the wearer. It also includes a running backpack, whose custom housing includes an onboard battery (Kobalt 24 V 2 Ah, Lowe's, Mooresville, NC, USA) and an NVIDIA Jetson Orin Nano (Jetson) computing platform. All sensors are fed through sewn-on cable channels to provide wired connections to the Jetson over a serial connection. The pant and insoles are available in multiple sizes and the wearable backpack can be adjusted to accommodate wearers of any size. The Jetson handles onboard and external communication and time synching between all sensors. It was selected for onboard use for its capability to run real-time deep learning models proficiently that could estimate biological joint angles and moments in real-time from wearable sensor data [29]. The overall system weighs about 2.1 kg but varies slightly depending on pant size, insole size, and cable lengths. The run time on a 2 Ah battery is about 4 hours and the design allows for hot-swapping of the batteries.

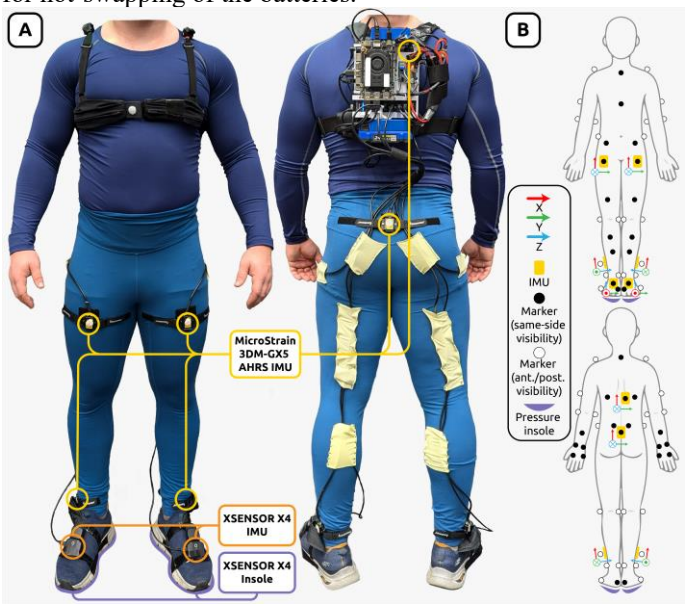

Fig 1. Second Skin and its onboard sensors. MicroStrain IMUs and XSENSOR X4 Sensor Pack each provided acceleration, angular velocity, and orientation. X4 insoles provided estimated normal force and bi-directional center of pressure. B. Mocap marker set and sensor locations and orientations.

Instructions for developing a replica of the Second Skin, the code-base needed to operate it, and instructions for operation can all be found in the Supplementary Materials, Section I.

B. Data Collection

We collected gait lab and wearable sensor data from 10 participants, all of whom were drawn from an able-bodied population (gender: 8 M, 2 F; age: 25.18 ± 3.12 years; body mass: 80.54 ± 12.56 kg; height: 1.75 ± 0.09 m). This study was approved by the Georgia Institute of Technology's Institutional Review Board (H21228), with all participants providing informed consent for the collection of experimental data. Each

Authorized licensed use limited to: Georgia Institute of Technology. Downloaded on October 31,2025 at 21:04:24 UTC from IEEE Xplore. Restrictions apply.
© 2025 IEEE. All rights reserved, including rights for text and data mining and training of artificial intelligence and similar technologies. Personal use is permitted, but republication/redistribution requires IEEE permission. See https://www.ieee.org/publications/rights/index.html for more information.

This article has been accepted for publication in IEEE Transactions on Biomedical Engineering. This is the author's version which has not been fully edited and content may change prior to final publication. Citation information: DOI 10.1109/TBME.2025.3589996

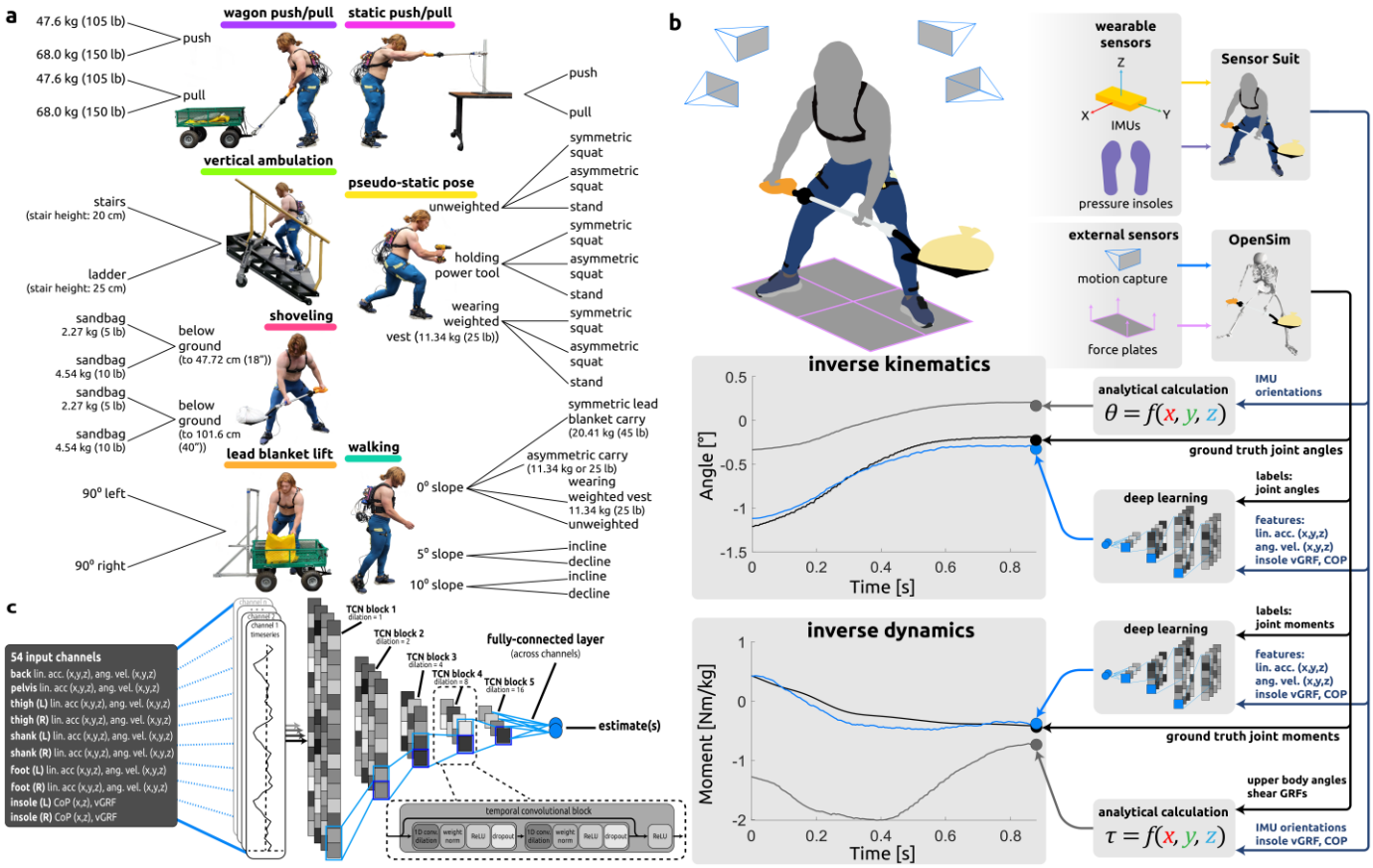

Fig 2. (A) Task set of 6 core activities consisting of 33 unique conditions: lead blanket lift (L), agon push/pull (PP), pseudo-static postures (PS), shoveling (SH), static push/pull (SP), vertical ambulation (VA), and walking (W). (B) Experimental data processing pipeline. Inverse kinematics and dynamics computed from mocap and force plate data through OpenSim served as ground truth reference values. Deep learning estimates and analytical calculations from wearable sensor data were compared to these ground truth data. Ground truth data was always filtered (6hz 4th order Butterworth) and all sensor data was spline interpolated to 200hz (already the sampling rate for Microstrain IMUs). The insole vGRFs were normalized to the wearer's bodyweight (C) Visual representation of the TCN architecture that was used including all input channels to the model.

individual performed a variety of tasks designed to mimic manual labor tasks at waste cleanup sites (Fig 2A). The types of tasks chosen were determined from incidence of injuries at these sites as well as feedback from workers on what tasks felt most strenuous. Then, we expanded on this taskset by adding in varied weight conditions, symmetry conditions, and incline conditions to make our dataset more diverse and broadly representative of human movement to facilitate more generalizable ML models. category had several sub-conditions of tasks performed. Most unique sub-conditions in the taskset were performed for either 5 or 10 repetitions, depending on complexity of the task, with participants completing each repetition at their own pace. The only exceptions to this were loaded walking, pseudo-static postures, and static pushing/pulling where each sub-condition was performed only once for 30 seconds. Force plate data, including vGRF and COP were recorded at 2000 Hz on an instrumented split-belt treadmill for walking trials and floor-embedded force plates for the rest of the task set (Bertec Corporation, Columbus OH, USA). Load cell data from an ATI mini45 (ATI Industrial Automation, NC, USA) were similarly sampled at 2000 Hz for shoveling, static push/pull, and wagon push/pull tasks to enable the calculation of reaction forces at the hands. Optical motion capture data were recorded at 200 Hz (Vicon Nexus, Vicon Motion Systems, Yarnton, Oxfordshire UK) using the marker set shown in Fig. 1B. MicroStrain IMUs were sampled at 200 Hz and the X4 sensor pack and X4 high-resolution insoles were sampled at 80 Hz. Wearable sensor data were synchronized with optical motion capture and force data using a Vicon lock box synchronization pin. The orientation data of the IMUs was tared before every task with the participant in a rehearsed neutral standing posture. Other than this taring process, no IMU calibration was performed. It is worth noting that IMU orientations were only used for analytically calculated joint states and not as features in the TCNs (Fig. 2.C). Thus, there was no calibration affecting any feature data in our TCNs.

We computed ground truth joint angles and moments from mocap, force plate, and load cell data using the inverse kinematics and inverse dynamics tools in OpenSim 4.0 [30] (Gait2392_Simbody model), with a 6 Hz Butterworth lowpass filter applied to mocap and force data. Although this model accounts for multiple degrees of freedom (DOFs) at the ankle, hip, and lower back, we restricted our analysis of joint kinematics and dynamics to just the sagittal plane component of the ankle, knee, hip, and lower back.

C. *Joint State Estimation Approach*

The machine learning algorithm implemented in this work to estimate lower-body joint angles and moments was a variant of the TCN originally developed by Bai et al. [31]. It was further

Authorized licensed use limited to: Georgia Institute of Technology. Downloaded on October 31,2025 at 21:04:24 UTC from IEEE Xplore. Restrictions apply.
© 2025 IEEE. All rights reserved, including rights for text and data mining and training of artificial intelligence and similar technologies. Personal use is permitted, but republication/redistribution requires IEEE permission. See https://www.ieee.org/publications/rights/index.html for more information.

This article has been accepted for publication in IEEE Transactions on Biomedical Engineering. This is the author's version which has not been fully edited and content may change prior to final publication. Citation information: DOI 10.1109/TBME.2025.3589996

developed by Molinaro et al. [32] for the purposes of biological moment estimation for hip/knee exoskeleton control. The TCN architecture benefitted from dilation between model layers, maximizing the effective time history used in the estimation of each successive time point while minimizing redundant network connections. To estimate the biological joint moments of cyclic and non-cyclic manual labor tasks, we trained TCN models with hyperparameters optimized for a similar able-bodied dataset comprising cyclic and non-cyclic tasks [32]. Here, the TCN was trained and tested in Python 3.6.9 using PyTorch 1.8.0 [33], using 5 temporal convolutional blocks. Each contained two convolutional layers with interstitial weight normalization and activation layers. The rectified linear unit (ReLU) was used as the activation function here for its previously demonstrated benefits in time series prediction implementations of deep learning models [34]. Each model was trained using the Adam optimizer and a mean squared error (MSE) loss function. We used a learning rate of 5e-5, dropout probability of 0.15, and 80 filters per hidden layer, corresponding to an effective time history of 248 points. Every model was trained and tested on the entire taskset from a random initialization with a ten-fold leave-one-subject-out validation for a maximum of 150 epochs and minimum of 75 epochs. We employed early stopping on model training if the validation loss increased for 20 consecutive epochs after the minimum 75 epochs were completed. A different model was trained for each withheld subject, for each of the 8 outcomes explored (sagittal joint angle and moment of the ankle, knee, hip, and lower back) and model performance was averaged across withheld subjects for each outcome. Orientation data from IMUs were not used as features, as we found that they did not improve model performance.

D. Load Cell Force Resolution

We used a pole instrumented with a 6-DOF load cell to quantify the reaction forces at the hands for wagon pushing/pulling, static pushing/pulling, and shoveling. To resolve the reaction forces at the right and left hands, the following system of equations were solved:

$$\sum F_{x,y,z} = F_{x,y,z}^{Loadcell} \qquad \sum M_{x,y,z} = M_{x,y,z}^{Loadcell} \tag{1}$$

An example of the expanded force and moment equations in the z-direction that provide every term involved in the calculation are fully written out below, to give an example of how this calculation was done. The most general form is provided, although some terms are later assumed to be zero.

$$F_z^{Right} + F_z^{Left} + F_z^{Load} = F_z^{Loadcell} \tag{2}$$

$$\begin{aligned}&(d_x^{Right} \text{ x } F_y^{Right}) + (d_y^{Right} \text{ x } F_x^{Right}) + \\ &(d_x^{Left} \text{ x } F_y^{Left}) + (d_y^{Left} \text{ x } F_x^{Left}) + (d_x^{Load} \text{ x } F_y^{Load}) + \\ &(d_y^{Load} \text{ x } F_x^{Load}) + M_z^{Right} + M_z^{Left} + M_z^{Load} = M_z^{Loadcell}\end{aligned} \tag{3}$$

Here, the superscripts *Right, Left,* and *Load* denote contributions from the right hand, left hand, and load, respectively. d denotes the distance from an applied force to the load cell, which was determined via optical motion capture data. To create a unique solution for this the system of equations described in (1), we assumed that moment and force were the same at the left and right hand for wagon pushing/pulling and static pushing/pulling due to the symmetric nature of the tasks. For shoveling, it was assumed that the force and moment at the left and right hand was the same through the axis of the pole (z-direction) and that neither hand exerted a moment in the x and y directions (Supplementary Materials, Section II).

E. Analytical Kinematics and Dynamics

In addition to training TCNs for angle and moment estimation, we analytically calculated joint angles and moments from raw sensor outputs to serve as a comparison metric for performance of the TCN models. For kinematics, sagittal plane angles were calculated by taking the difference in segment angles of two IMUs across a joint. Our IMUs came with stock calibrations and robust onboard filters for pose estimation, which we operated with the magnetometer disabled to avoid magnetic noise in our collection space from corrupting each IMU's pose estimate. To calculate joint moments, IMU-derived lower-body joint angles, normal force from the pressure insoles, and COP from the pressure insoles were substituted in for lower body inverse kinematics from optical motion capture, normal force measured by force plates, and COP measured by force plates, respectively. Then, these inputs were run through the inverse dynamics tool in OpenSim. Ground truth upper body joint angles, shear reaction forces and moments, and model scaling properties from a full optical motion capture set were still used for this calculation to create a 'best case' calculation against which to compare TCN results, as our system does not have a corresponding measurement to these key inputs to inverse dynamics analysis. We allowed the analytical approach to 'cheat' in this way to demonstrate the performance of the deep learning system against the absolute best-case of the analytical system; in reality, its performance would be worse than what is reported here.

F. Outcome Metrics

We used RMSE and R^2 to assess model performance throughout the paper. All timeseries data (ground truth, analytical estimates, and ML estimates) were filtered with a 4th order 6 Hz Butterworth filter before computing RMSE and R^2 between estimates and ground truth. Every task-specific outcome calculation only includes data for that task. For example, RMSE of *SH* only includes shoveling data, but RMSE of *Overall* includes all tasks in the dataset. RMSE is calculated by first taking the mean squared error (MSE) across all datapoints in all timeseries data relevant to the task being assessed and then calculating its square root to get RMSE. R^2 is calculated on a trial-by-trial basis for each task being assessed. The Pearson's correlation coefficient is calculated between estimate and ground truth for every relevant trial, then squared to get the R^2 value for each trial. Lastly, the R^2 value from each trial is averaged to get the final R^2 metric for each outcome.

G. Statistical Analysis

MATLAB 2024a (Mathworks, Natick, MA, USA) was used to perform a one-way repeated measures ANOVA test ($\alpha = .05$) for all 8 outcome types (joint moment and angle of the lower back, hip, knee and ankle) for both outcome metrics (R^2 and

Authorized licensed use limited to: Georgia Institute of Technology. Downloaded on October 31,2025 at 21:04:24 UTC from IEEE Xplore. Restrictions apply.
© 2025 IEEE. All rights reserved, including rights for text and data mining and training of artificial intelligence and similar technologies. Personal use is permitted, but republication/redistribution requires IEEE permission. See https://www.ieee.org/publications/rights/index.html for more information.

This article has been accepted for publication in IEEE Transactions on Biomedical Engineering. This is the author's version which has not been fully edited and content may change prior to final publication. Citation information: DOI 10.1109/TBME.2025.3589996

RMSE), for all task types collected to determine the statistical significance of differences between ML-based and analytical

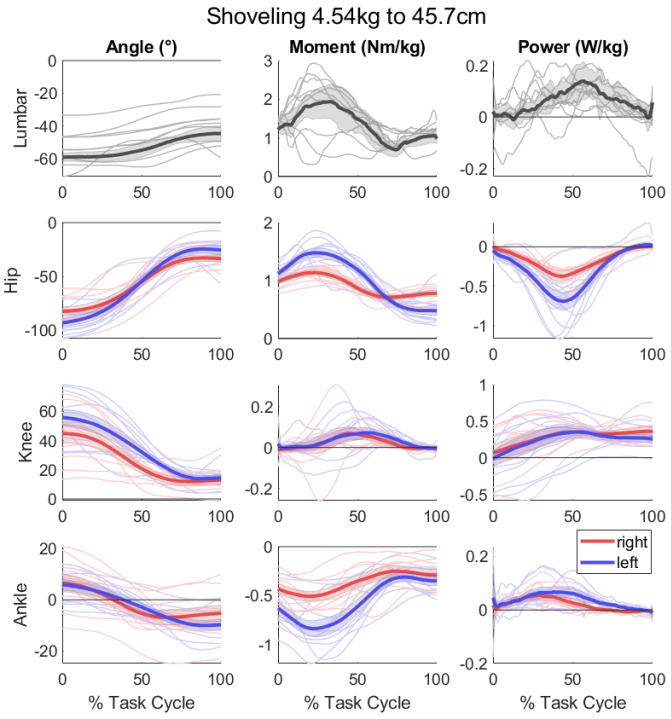

Fig 3. Overall and individual participant averages of joint angle, normalized joint moment, and normalized joint power for the lumbar, hip, knee, and ankle, for shoveling 4.54kg (10lb) to 45.7cm (18").

tracking of joint state. The predictor variable was model type (ML vs analytical). Each participant was treated as a separate measure, making this a within-subjects statistical analysis. Mauchly's sphericity test ($\alpha = .05$) was used to verify the sphericity assumption of data before performing every ANOVA test.

III. Results

A. Novel Biomechanics

Because the taskset described in Fig. 2A features many tasks which are not commonly reported in the biomechanics literature, a visualization of ground truth biomechanical time-series data of one of those tasks is provided in Fig. 3, for shoveling 4.54 kg (10 lbs) to 45.7 cm (18"). Overall participant averages and individual participant averages are shown for joint angle, normalized joint moment, and normalized joint power of left and right ankle flexion, left and right knee flexion, left and right hip flexion, and lumbar flexion. Red and blue represent the right and left joint, respectively, for bilateral joints. Time series visualizations for lead blanket lifting and ladder ascent and descent can be found in the Supplement, Section IV. This section also contains a link to the biomechanics dataset for this study which includes wearable sensor data, EMG, motion capture data, rection force data, inverse kinematics data, and inverse dynamics data from all tasks for the full N=10 subjects collected for this study.

B. Ground Reaction Forces

Fig 4a. shows the Second Skin's R^2 and RMSE values for GRF tracking. Normal force, frontal COP, and lateral COP had RMSE values of .146±.022 bodyweights, .102±.009 foot-lengths, and .096±.013 foot-widths, respectively, across all participants and tasks. Walking had the highest RMSE values of every task type for normal force (.235±.084 bodyweights), frontal COP (.141±.015 foot-lengths), and lateral COP (.171±.096 foot-widths). Pseudo-static postures and static push/pull both had abnormally low R^2 values for normal force tracking (.438±.039 and .406±.093, respectively), while maintaining RMSE values in-line with other tasks due to the

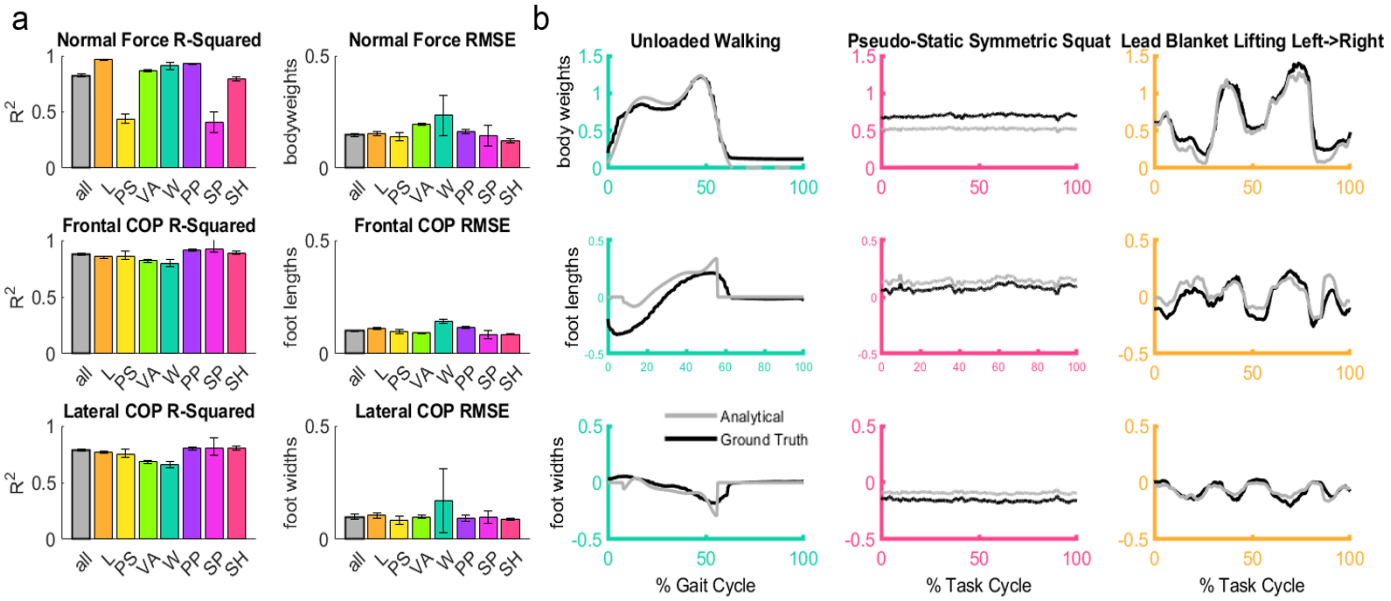

Fig 4. (a) R^2 and RMSE of normal force, frontal COP, and lateral COP tracking across all tasks. (b) Kinetic timeseries data from a representative participant

Authorized licensed use limited to: Georgia Institute of Technology. Downloaded on October 31,2025 at 21:04:24 UTC from IEEE Xplore. Restrictions apply.
© 2025 IEEE. All rights reserved, including rights for text and data mining and training of artificial intelligence and similar technologies. Personal use is permitted, but republication/redistribution requires IEEE permission. See https://www.ieee.org/publications/rights/index.html for more information.

This article has been accepted for publication in IEEE Transactions on Biomedical Engineering. This is the author's version which has not been fully edited and content may change prior to final publication. Citation information: DOI 10.1109/TBME.2025.3589996

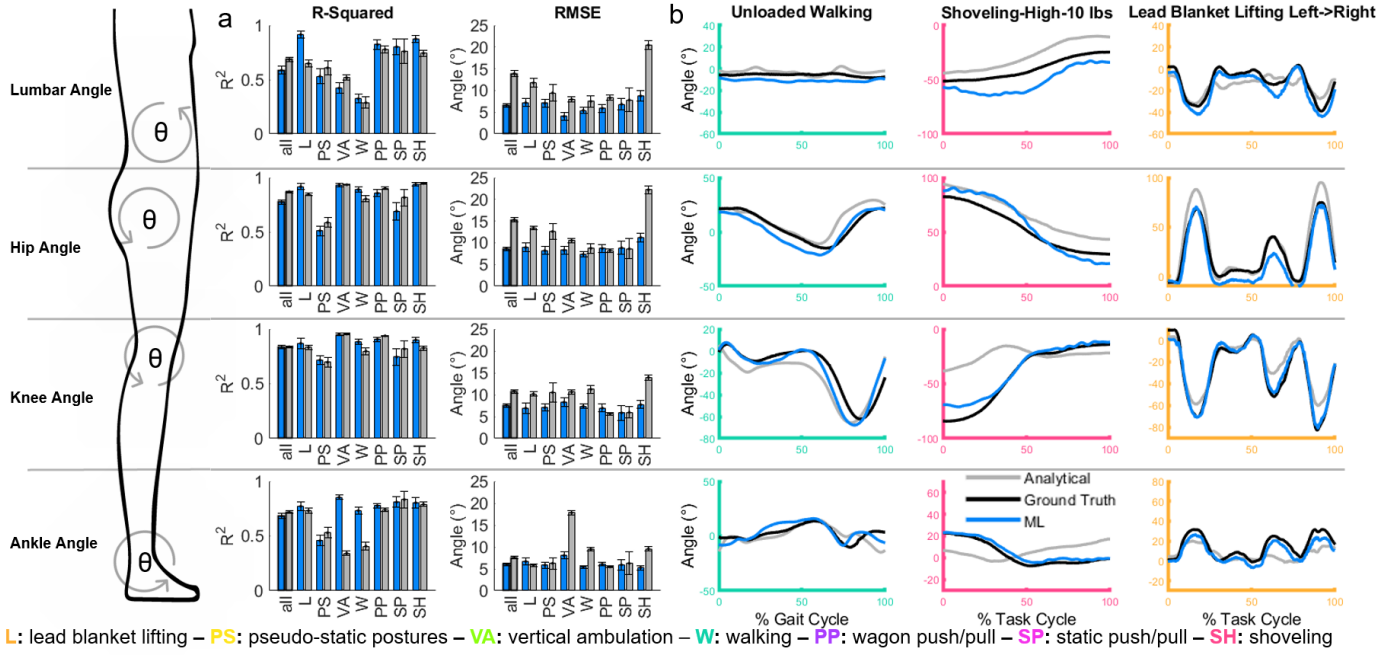

Fig 5. (a) R^2 and RMSE of lumbar, hip, knee, and ankle kinematics from both TCN estimates and analytically derived estimates. (b) Kinematic timeseries data from a representative participant

isometric-like nature of these tasks. Fig 2b. column 2 shows the timeseries GRF tracking of one of these tasks and should help to visualize why the R^2 value is poor for these tasks, as there is essentially no trend in the data, making correlation fitting a difficult metric for model performance on these tasks. The phenomenon of low R^2 values yet in-line RMSE values for Pseudo-static postures and static push/pull exists for kinematic tracking (Fig 5a.) and moment tracking (Fig 6a.) as well.

C. *Kinematics*

Fig 5a. shows R^2 and RMSE values of analytically derived and TCN derived estimates of sagittal plane joint angles. The TCN estimates had significantly lower overall RMSE than the analytically derived joint kinematics at every joint except the ankle ($p < .05$) with the most extreme case being a relative RMSE reduction of over 50% at the lower back. At the ankle, TCN estimate RMSE was significantly lower than analytically derived RMSE for vertical ambulation, walking, wagon push/pull and shoveling ($p < .05$). Analytically derived RMSE was not significantly lower than TCN RMSE for kinematics of any task types at any joint. The RMSE for analytical joint angle tracking of shoveling at the lower back stands out as being much higher than RMSE for the rest of the tasks. This is because the lower back and hip experience higher flexion angles during shoveling than the rest of the taskset. The same

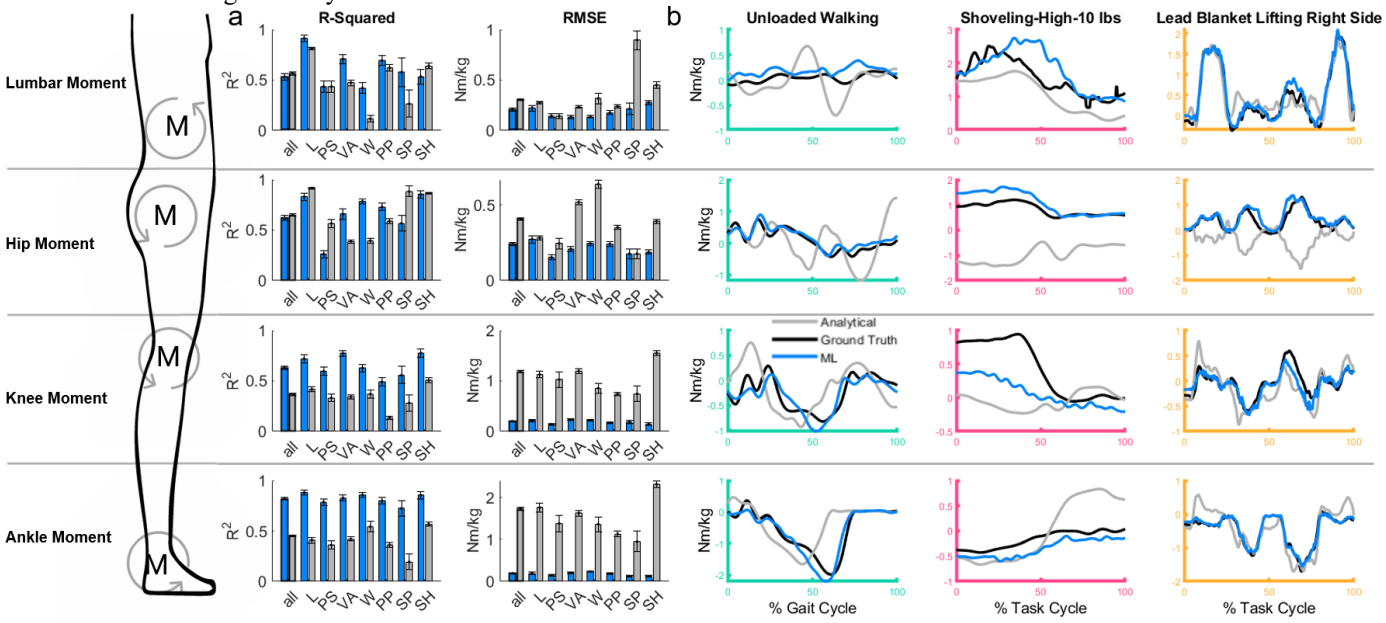

Fig 6. (a) R^2 and RMSE of lumbar, hip, knee, and ankle moments from both TCN estimates and analytically derived estimates. (b) Joint moment timeseries data from a representative participant containing ground truth joint moment, analytically derived joint moment, and TCN estimates of joint moment.

Authorized licensed use limited to: Georgia Institute of Technology. Downloaded on October 31,2025 at 21:04:24 UTC from IEEE Xplore. Restrictions apply.
© 2025 IEEE. All rights reserved, including rights for text and data mining and training of artificial intelligence and similar technologies. Personal use is permitted, but republication/redistribution requires IEEE permission. See https://www.ieee.org/publications/rights/index.html for more information.

This article has been accepted for publication in IEEE Transactions on Biomedical Engineering. This is the author's version which has not been fully edited and content may change prior to final publication. Citation information: DOI 10.1109/TBME.2025.3589996

trend can be seen for vertical ambulation at the ankle, which is by far the task with the most ankle flexion in our taskset. R^2 tracking for walking at the lower back is another task with an abnormal performance relative to other tasks. This is because the lower back angle is essentially constant during walking (fig 5b., column 1), making this another instance of a task within our taskset where RMSE is normal, but R^2 is a very difficult metricfor a model to uphold.

D. Joint Moments

Fig 6a. shows R^2 and RMSE values of analytically derived and TCN derived estimates of normalized joint moments. Overall RMSE of TCN moment estimates at the lower back, hip, knee, and ankle were .207±.069 Nm/kg, .242±.044 Nm/kg, .202±.038 Nm/kg, and .193±.034 Nm/kg, respectively. The TCN estimates had significantly lower overall RMSE than the analytically derived moments for every task at every joint ($p < .05$). The worst performance of TCN estimates by a wide margin was at the lower back for shoveling (.295±.093 Nm/kg) where there were significant reaction forces at the hands that the Second Skin is not equipped to directly sense. This can be seen within timeseries data from the representative participant (Fig. 6b.). Overall RMSE of analytically derived joint moments at the lower back, hip, knee, and ankle were .306±.036 Nm/kg, .407±.021 Nm/kg, 1.18 ±.022 Nm/kg, and 1.73±.071 Nm/kg, respectively.

IV. Discussion

A. ML vs. Analytical Estimates of Body-Joint Dynamics

Our main hypothesis that deep learning-based body-joint state estimates outperform analytically derived joint states was overwhelmingly supported (Figs. 5,6). There were no joint states for any task type where analytically derived joint states had significantly lower RMSE than TCN estimates. Furthermore, the only joint state that the TCN did not have significantly lower overall RMSE values for was ankle angle, and only in a few tasks. The industry standard of analytical, wearable kinematic tracking was XSens's MVN system circa 2020, before they decided to adopt heavier ML practices for kinematic tracking as well. Our TCN estimates of joint angles likewise outperform this system, with angle RMSEs of 6.0°, 7.6°, and 8.6° compared to 6.8°, 9.6°, and 8.6° at the ankle, knee and hip, respectively [35].

Even with some of the best MEMS IMUs available currently, combined with a highly accurate pressure insole (as seen by our results in Fig. 4), and providing ground truth values for shear forces and twist-axis moments, analytical inverse dynamics is far too inaccurate for real-world deployment (Fig. 6). However, we believe the results presented here show that incorporating end-to-end deep learning, thereby eliminating challenges associated with shear sensing, and avoiding an approach prone to error propagation, can lead to reasonable inverse dynamics that are user-independent and task-agnostic (e.g. highly generalizable). Few studies have validated generalizability to the extent shown here.

B. Second Skin Sensing Performance vs. State of the Art

Figueiredo et al. achieved R^2 values of .92, .94, and .87 for sagittal hip, knee, and ankle angles, respectively, during walking [28], compared to our R^2 values of .94, .96, and .82 on our walking tasks. However, our system did not rely on precise sensor placement and task-specific models. Hernandez et al. was able to achieve mean absolute errors (MAE) for walking and running of 3.7°, 2.9°, and 5.1° at the hip, knee, and ankle, respectively, without relying on precise sensor placement [36]. This slightly outperforms our MAE for walking of 6.1°, 4.8°, and 4.3° at the hip, knee, and ankle, however they included a significantly larger and more homogeneous population of 27 males, with no females and only had to perform well on two gaits. Overall, we believe our system performed in line with current *wearable* state-of-the-art for kinematic sensing as we have accuracy that is closely in line with the very best presented in the literature and demonstrate generalization of our system on a far wider task set than shown previously.

Where our system is truly novel is its ability to estimate joint moments in a task-agnostic, subject-independent manner. The only other system to have implemented this successfully is Molinaro et al. [32]. Molinaro et al. achieved RMSE of .15 Nm/kg and .13 Nm/kg for cyclic tasks and .21 Nm/kg and .16 Nm/kg for non-cyclic tasks at the hip and knee, respectively. This is compared to our result of .22 Nm/kg and .22 Nm/kg for walking and .21 Nm/kg and .17 Nm/kg for non-cyclic tasks at the hip and knee, respectively. We were slightly outperformed in terms of RMSE in walking, but had nearly the same for non-cyclic tasking. Our results interestingly show worse results for cyclic tasks than non-cyclic tasks, which is contrary to what Molinaro et al. observed. We believe this is due to our dataset having very little cyclical data compared to the dataset used in Molinaro et al. (Fig. 4b). It is worth noting that our system has two key advantages over Molinaro et al. which its functionality at more joints (ankle and lower back), and the fact that it was designed to be a sensing suite that is reasonably compatible with biofeedback systems and wearable robots. Additionally, our sensors were on the human body (rather than on an exoskeleton) allowing for deployability across different wearable devices, as well as to contexts outside wearable robotics such as biofeedback training and out-of-the-lab biomechanics collections.

C. Challenges for Analytical Inverse Dynamics in Wearables

Our analytically derived inverse dynamics results show increasingly worse performance moving proximally from the ground. We believe this is due to kinematic error propagating from joint to joint, which is not an issue experienced in our end-to-end deep learning approach. A similar trend is seen in the work of both Liu et al. and Khurelbaatar et al. where inverse dynamics and kinematics are solved from the ground up, and dynamics error propagates in the same direction [18],[19]. In these analyses, however, optical kinematic tracking is employed, which cuts down heavily on kinematic error. This suggests that with the current *wearable* state-of-the-art for kinematic tracking, analytical methods for ground up inverse dynamics alone may be insufficient. Perhaps other analytical models, like top-down approaches could be considered for analytical models of proximal joints (like the back and hip) [37], but this was beyond the scope of this study.

Authorized licensed use limited to: Georgia Institute of Technology. Downloaded on October 31,2025 at 21:04:24 UTC from IEEE Xplore. Restrictions apply.
© 2025 IEEE. All rights reserved, including rights for text and data mining and training of artificial intelligence and similar technologies. Personal use is permitted, but republication/redistribution requires IEEE permission. See https://www.ieee.org/publications/rights/index.html for more information.

This article has been accepted for publication in IEEE Transactions on Biomedical Engineering. This is the author's version which has not been fully edited and content may change prior to final publication. Citation information: DOI 10.1109/TBME.2025.3589996

D. Limitations

The Second Skin itself lacks inertial sensors at the arms and has kinetic sensors only at the feet. This limits its capabilities to lower-body biomechanics only and requires users to be on their feet to attain reasonable joint moment estimates. Future iterations of our open-source Second Skin platform will address these limitations as arm forces are also critical for monitoring many industrial tasks, such as some of the ones collected in this protocol.

Certain tasks in our dataset had reaction forces at the hands, for which we had to make assumptions to fully characterize from a single load-cell. This likely introduced a small amount of error into our 'ground truth' inverse dynamics results for these tasks. However, these rection forces were characterized reasonably well, they were typically at least an order of magnitude smaller than the ground reaction forces, and they were applied to the body at distal locations relative to all the joints of interest in our analysis. It is therefore unlikely that this limitation had a significant impact on our results.

The experiment conducted was designed to stay within the scope of tasks commonly performed by industrial workers and thus is not perfectly representative of all the tasks that a person may perform while wearing the Second Skin. For example, high power movements such as running and jumping are absent from the taskset, so it is unclear how the Second Skin would perform in these cases with the current existing models. However, the performance of the task-agnostic models we trained across the plethora of tasks that were included suggests that the Second Skin is capable of good performance across an incredibly diverse range of tasks. We therefore believe that this work, and the robustness of the Second Skin could be seamlessly expanded to new biomechanical domains outside the realm of manual labor, so long as there is sufficient data to train new models.

The population of the dataset collected was entirely able bodied, with ages ranging from 22 to 32 years old, and included only 2 female participants. It is thus unclear if the Second Skin would produce reliable biomechanics estimates on clinical populations and for people significantly out of this age range. Furthermore, it is unclear if there is a significant difference between model performance on males and females, and if separate male and female models should be considered.

Our dataset was only about half the size of the dataset collected by Molinaro et al. [32], and we have nearly twice as many timeseries channels of input to our model. Because more data are generally needed for models to perform optimally when they have more inputs [38], our system may have been limited by the amount of data that we had, or conversely the amount of sensor channels we chose to include for each joint state estimation model. In future work, the Second Skin's performance will likely benefit from more data, a formal analysis on feature importance for each joint state, and a hyperparameter optimization of its own, rather than using Molinaro's extensive hyperparameter optimization results, which requires an extremely large amount of compute resources.

V. Conclusion

This study investigated a novel, participant-independent, task-agnostic approach for estimating joint angle and moment at the lower back, hip, knee, and ankle, the design and software for which was made open-source. We demonstrated that with a large and diverse dataset, deep learning can enable fast and accurate estimates of human kinematics and dynamics. Our system achieved competitive performance with previous machine learning and analytical-based kinematic and dynamics wearable sensing systems within the literature, and did so while generalizing to a diverse array of tasks and joint states. We were able to reliably estimate joint moments in a subject-independent and task-agnostic manner, even for tasks with reaction forces at the hands (shoveling, wagon push/pull, static push/pull), which were extremely challenging tasks for analytical-based solutions. In the future, this work should be expanded on with larger datasets and more optimized model training to improve accuracy and generalization further to move towards real-world deployment efforts. This approach to wearable sensing has the potential to revolutionize biomechanics as it could allow for a far more accessible means of collecting data that requires less post-processing, while simultaneously allowing for more natural movement patterns than current biomechanics labs. Likewise, this framework could expand the capabilities of biofeedback systems and wearable robots by enabling better real-time sensing and control.

Acknowledgment

This work was funded by the US Department of Energy's Office of Environmental Management. We would like to thank Jennifer Leestma, Dongho Park, Siddharth Nathella, and Taryn Harvey, all of whom aided in the software and hardware design of the Second Skin. We would also like to thank all the participants who took part in this study.

Sandia National Laboratories is a multi-mission laboratory managed and operated by National Technology & Engineering Solutions of Sandia, LLC (NTESS), a wholly owned subsidiary of Honeywell International Inc., for the U.S. Department of Energy's National Nuclear Security Administration (DOE/NNSA) under contract DE-NA0003525. This written work is authored by an employee of NTESS. The employee, not NTESS, owns the right, title and interest in and to the written work and is responsible for its contents. Any subjective views or opinions that might be expressed in the written work do not necessarily represent the views of the U.S. Government. The publisher acknowledges that the U.S. Government retains a non-exclusive, paid-up, irrevocable, world-wide license to publish or reproduce the published form of this written work or allow others to do so, for U.S. Government purposes. The DOE will provide public access to results of federally sponsored research in accordance with the DOE Public Access Plan

References

[1] S. P. Schneider, "Musculoskeletal injuries in construction: a review of the literature," *Appl. Occup. Environ. Hyg.*, vol. 16, no. 11, pp. 1056–1064, Nov. 2001, doi: 10.1080/104732201753214161.

[2] R. Jabbour, S. Turner, L. Hussey, F. Page, and R. Agius, "Workplace injury data reported by occupational physicians and general

Authorized licensed use limited to: Georgia Institute of Technology. Downloaded on October 31,2025 at 21:04:24 UTC from IEEE Xplore. Restrictions apply.
© 2025 IEEE. All rights reserved, including rights for text and data mining and training of artificial intelligence and similar technologies. Personal use is permitted, but republication/redistribution requires IEEE permission. See https://www.ieee.org/publications/rights/index.html for more information.

This article has been accepted for publication in IEEE Transactions on Biomedical Engineering. This is the author's version which has not been fully edited and content may change prior to final publication. Citation information: DOI 10.1109/TBME.2025.3589996

practitioners," *Occup. Med. Oxf. Engl.*, vol. 65, no. 4, pp. 296–302, Jun. 2015, doi: 10.1093/occmed/kqv014.

[3] J. Theurel and K. and Desbrosses, "Occupational Exoskeletons: Overview of Their Benefits and Limitations in Preventing Work-Related Musculoskeletal Disorders," *IISE Trans. Occup. Ergon. Hum. Factors*, vol. 7, no. 3–4, pp. 264–280, Oct. 2019, doi: 10.1080/24725838.2019.1638331.

[4] [1] C. Wong, Z.-Q. Zhang, B. Lo, and G.-Z. Yang, "Wearable Sensing for Solid Biomechanics: A Review," *IEEE Sens. J.*, vol. 15, no. 5, pp. 2747–2760, May 2015, doi: 10.1109/JSEN.2015.2393883.

[5] D. T.-P. Fong and Y.-Y. Chan, "The Use of Wearable Inertial Motion Sensors in Human Lower Limb Biomechanics Studies: A Systematic Review," *Sensors*, vol. 10, no. 12, Art. no. 12, Dec. 2010, doi: 10.3390/s101211556.

[6] D. G. E. Robertson, G. E. Caldwell, J. Hamill, G. Kamen, and S. Whittlesey, *Research Methods in Biomechanics*. Human Kinetics, 2013.

[7] Y. Menguc *et al.*, "Soft Wearable Motion Sensing Suit for Lower Limb Biomechanics Measurements."

[8] G. Frediani, B. Botondi, L. Quartini, G. Zonfrillo, L. Bocchi, and F. Carpi, "Wearable Kinematic Monitoring System Based on Piezocapacitive Sensors," *Stud. Health Technol. Inform.*, vol. 261, pp. 103–108, 2019.

[9] P. Slade, A. Habib, J. L. Hicks, and S. L. Delp, "An Open-Source and Wearable System for Measuring 3D Human Motion in Real-Time," *IEEE Trans. Biomed. Eng.*, vol. 69, no. 2, pp. 678–688, Feb. 2022, doi: 10.1109/TBME.2021.3103201.

[10] L. Sy *et al.*, "Estimating Lower Limb Kinematics Using a Reduced Wearable Sensor Count," *IEEE Trans. Biomed. Eng.*, vol. 68, no. 4, pp. 1293–1304, Apr. 2021, doi: 10.1109/TBME.2020.3026464.

[11] J. L. McGinley, R. Baker, R. Wolfe, and M. E. Morris, "The reliability of three-dimensional kinematic gait measurements: a systematic review," *Gait Posture*, vol. 29, no. 3, pp. 360–369, Apr. 2009, doi: 10.1016/j.gaitpost.2008.09.003.

[12] T. S. Buchanan, D. G. Lloyd, K. Manal, and T. F. Besier, "Estimation of Muscle Forces and Joint Moments Using a Forward-Inverse Dynamics Model," *Med. Sci. Sports Exerc.*, vol. 37, no. 11, p. 1911, Nov. 2005, doi: 10.1249/01.mss.0000176684.24008.6f.

[13] M. Sartori, M. Reggiani, D. Farina, and D. G. Lloyd, "EMG-Driven Forward-Dynamic Estimation of Muscle Force and Joint Moment about Multiple Degrees of Freedom in the Human Lower Extremity," *PLOS ONE*, vol. 7, no. 12, p. e52618, Dec. 2012, doi: 10.1371/journal.pone.0052618.

[14] D. Staudenmann, I. Kingma, A. Daffertshofer, D. F. Stegeman, and J. H. van Dieën, "Improving EMG-based muscle force estimation by using a high-density EMG grid and principal component analysis," *IEEE Trans. Biomed. Eng.*, vol. 53, no. 4, pp. 712–719, Apr. 2006, doi: 10.1109/TBME.2006.870246.

[15] Q. Shao, D. N. Bassett, K. Manal, and T. S. Buchanan, "An EMG-driven model to estimate muscle forces and joint moments in stroke patients," *Comput. Biol. Med.*, vol. 39, no. 12, pp. 1083–1088, Dec. 2009, doi: 10.1016/j.compbiomed.2009.09.002.

[16] U. J. Naeem, C. Xiong, and A. A. Abdullah, "EMG-muscle force estimation model based on back-propagation neural network," *2012 IEEE Int. Conf. Virtual Environ. Hum.-Comput. Interfaces Meas. Syst. VECIMS Proc.*, 2012, Accessed: Aug. 20, 2024. [Online]. Available: https://www.semanticscholar.org/paper/EMG-muscle-force-estimation-model-based-on-neural-Naeem-Xiong/1345379d1c54d764fdf7f353e5de0b88bf25b654

[17] D. A. Jacobs and D. P. Ferris, "Estimation of ground reaction forces and ankle moment with multiple, low-cost sensors," *J. NeuroEngineering Rehabil.*, vol. 12, no. 1, p. 90, Oct. 2015, doi: 10.1186/s12984-015-0081-x.

[18] T. Khurelbaatar, K. Kim, S. Lee, and Y. H. Kim, "Consistent accuracy in whole-body joint kinetics during gait using wearable inertial motion sensors and in-shoe pressure sensors," *Gait Posture*, vol. 42, no. 1, pp. 65–69, Jun. 2015, doi: 10.1016/j.gaitpost.2015.04.007.

[19] T. Liu, Y. Inoue, K. Shibata, K. Shiojima, and M. M. Han, "Triaxial joint moment estimation using a wearable three-dimensional gait analysis system," *Measurement*, vol. 47, pp. 125–129, Jan. 2014, doi: 10.1016/j.measurement.2013.08.020.

[20] C. Wang *et al.*, "Real-Time Estimation of Knee Adduction Moment for Gait Retraining in Patients With Knee Osteoarthritis," *IEEE Trans. Neural Syst. Rehabil. Eng.*, vol. 28, no. 4, pp. 888–894, Apr. 2020, doi: 10.1109/TNSRE.2020.2978537.

[21] X. Jiang, M. Gholami, M. Khoshnam, J. J. Eng, and C. Menon, "Estimation of Ankle Joint Power during Walking Using Two Inertial Sensors," *Sensors*, vol. 19, no. 12, Art. no. 12, Jan. 2019, doi: 10.3390/s19122796.

[22] G. Ding, I. Georgilas, and A. Plummer, "A Deep Learning Model with a Self-Attention Mechanism for Leg Joint Angle Estimation across Varied Locomotion Modes," *Sensors*, vol. 24, no. 1, Art. no. 1, Jan. 2024, doi: 10.3390/s24010211.

[23] M. Mundt, W. R. Johnson, W. Potthast, B. Markert, A. Mian, and J. Alderson, "A Comparison of Three Neural Network Approaches for Estimating Joint Angles and Moments from Inertial Measurement Units," *Sensors*, vol. 21, no. 13, Art. no. 13, Jan. 2021, doi: 10.3390/s21134535.

[24] F. Wang *et al.*, "Estimation of Lower Limb Joint Angles and Joint Moments during Different Locomotive Activities Using the Inertial Measurement Units and a Hybrid Deep Learning Model," *Sensors*, vol. 23, no. 22, Art. no. 22, Jan. 2023, doi: 10.3390/s23229039.

[25] Y. Zhu, D. Xia, and H. Zhang, "Using Wearable Sensors to Estimate Vertical Ground Reaction Force Based on a Transformer," *Appl. Sci.*, vol. 13, no. 4, Art. no. 4, Jan. 2023, doi: 10.3390/app13042136.

[26] S. Chae, A. Choi, H. Jung, T. H. Kim, K. Kim, and J. H. Mun, "Machine Learning Model to Estimate Net Joint Moments during Lifting Task Using Wearable Sensors: A Preliminary Study for Design of Exoskeleton Control System," *Appl. Sci.*, vol. 11, no. 24, Art. no. 24, Jan. 2021, doi: 10.3390/app112411735.

[27] D. D. Molinaro, I. Kang, J. Camargo, M. C. Gombolay, and A. J. Young, "Subject-Independent, Biological Hip Moment Estimation During Multimodal Overground Ambulation Using Deep Learning," *IEEE Trans. Med. Robot. Bionics*, vol. 4, no. 1, pp. 219–229, Feb. 2022, doi: 10.1109/TMRB.2022.3144025.

[28] J. Figueiredo, S. P. Carvalho, J. P. Vilas-Boas, L. M. Gonçalves, J. C. Moreno, and C. P. Santos, "Wearable Inertial Sensor System towards Daily Human Kinematic Gait Analysis: Benchmarking Analysis to MVN BIOMECH," *Sensors*, vol. 20, no. 8, Art. no. 8, Jan. 2020, doi: 10.3390/s20082185.

[29] D. D. Molinaro, I. Kang, and A. J. Young, "Estimating human joint moments unifies exoskeleton control, reducing user effort," *Sci. Robot.*, vol. 9, no. 88, p. eadi8852, Mar. 2024, doi: 10.1126/scirobotics.adi8852.

[30] S. L. Delp *et al.*, "OpenSim: Open-Source Software to Create and Analyze Dynamic Simulations of Movement," *IEEE Trans. Biomed. Eng.*, vol. 54, no. 11, pp. 1940–1950, Nov. 2007, doi: 10.1109/TBME.2007.901024.

[31] S. Bai, J. Z. Kolter, and V. Koltun, "An Empirical Evaluation of Generic Convolutional and Recurrent Networks for Sequence Modeling," Apr. 19, 2018, *arXiv*: arXiv:1803.01271. Accessed: Aug. 20, 2024. [Online]. Available: http://arxiv.org/abs/1803.01271

[32] D. D. Molinaro, K. Scherpereel, E. B. Schonhaut, G. Evangelopoulos, M. K. Shepherd, and A. J. Young, "Task-Agnostic Exoskeleton Control via Biological Joint Moment Estimation," *Nature*, vol. (In Press), 2024.

[33] A. Paszke *et al.*, "PyTorch: An Imperative Style, High-Performance Deep Learning Library," in *Advances in Neural Information Processing Systems*, Curran Associates, Inc., 2019. Accessed: Oct. 10, 2023. [Online]. Available: https://papers.nips.cc/paper_files/paper/2019/hash/bdbca288fee7f92f2bfa9f7012727740-Abstract.html

[34] X. Glorot, A. Bordes, and Y. Bengio, "Deep Sparse Rectifier Neural Networks," in *Proceedings of the Fourteenth International Conference on Artificial Intelligence and Statistics*, JMLR Workshop and Conference Proceedings, Jun. 2011, pp. 315–323. Accessed: Oct. 10, 2023. [Online]. Available: https://proceedings.mlr.press/v15/glorot11a.html

[35] M. P. Mavor, G. B. Ross, A. L. Clouthier, T. Karakolis, and R. B. Graham, "Validation of an IMU Suit for Military-Based Tasks," *Sensors*, vol. 20, no. 15, Art. no. 15, Jan. 2020, doi: 10.3390/s20154280.

[36] V. Hernandez, D. Dadkhah, V. Babakeshizadeh, and D. Kulić, "Lower body kinematics estimation from wearable sensors for walking and running: A deep learning approach," *Gait Posture*, vol. 83, pp. 185–193, Jan. 2021, doi: 10.1016/j.gaitpost.2020.10.026.

[37] Y. Iino and T. Kojima, "Validity of the top-down approach of inverse dynamics analysis in fast and large rotational trunk movements," *J. Appl. Biomech.*, vol. 28, no. 4, pp. 420–430, Aug. 2012, doi: 10.1123/jab.28.4.420.

[38] M. I. Jordan and T. M. Mitchell, "Machine learning: Trends, perspectives, and prospects," *Science*, vol. 349, no. 6245, pp. 255–260, Jul. 2015, doi: 10.1126/science.aaa841

Authorized licensed use limited to: Georgia Institute of Technology. Downloaded on October 31,2025 at 21:04:24 UTC from IEEE Xplore. Restrictions apply.
© 2025 IEEE. All rights reserved, including rights for text and data mining and training of artificial intelligence and similar technologies. Personal use is permitted, but republication/redistribution requires IEEE permission. See https://www.ieee.org/publications/rights/index.html for more information.

This article has been accepted for publication in IEEE Transactions on Biomedical Engineering. This is the author's version which has not been fully edited and content may change prior to final publication. Citation information: DOI 10.1109/TBME.2025.3589996

Authorized licensed use limited to: Georgia Institute of Technology. Downloaded on October 31,2025 at 21:04:24 UTC from IEEE Xplore. Restrictions apply.
© 2025 IEEE. All rights reserved, including rights for text and data mining and training of artificial intelligence and similar technologies. Personal use is permitted, but republication/redistribution requires IEEE permission. See https://www.ieee.org/publications/rights/index.html for more information.